Mean-field polariton theory for asymmetric quantum wells

R. Atanasov and F. Bassani
Scuola Normale Superiore, Piazza dei Cavalieri-7, I-56126 Pisa, Italy

V. M. Agranovich
Institute of Spectroscopy, Russian Academy of Science, Troitsk, Moscow oblast, Russia
(Received 18 May 1993)

We present a simple method to compute the optical properties of quantum wells of any shape, using microscopic calculations of the electronic states. Near the exciton resonances simple expressions for the polariton states and the radiative lifetimes are obtained as functions of the in-plane wave vector $K_{\parallel}$. The cases of a GaAs/Al$_x$Ga$_{1-x}$As/AlAs asymmetric well and of double wells are considered; the results relate to those of the symmetric well. The computed splitting between the Z mode and the T mode is shown to depend mostly on the thickness, in fair agreement with experiments by Fröhlich *et al.* Polaritons associated with crossed excitons involving pairs of subbands forbidden in the symmetric case are found, and are shown to give rise to additional structure in the reflectivity.

I. INTRODUCTION

The problem of the optical response of a composite medium containing mesoscopic structures, such as thin layers, superlattices, quantum wires, or quantum dots, is of current interest. New excitonic and polaritonic effects have been observed in connection with the electronic excitations of the confined states in multiple quantum wells (QW's) and superlattices (SL's),[1-3] quantum well wires (QWW's),[4,5] and semiconductor slabs.[6] For the case of multiple QW's and QWW's the theory of polariton states has been considered by solving Maxwell equations with a nonlocal susceptibility,[7,8] and also by using a second quantization formalism with the $\mathbf{A}\cdot\mathbf{p}$ interaction in the Hamiltonian.[9] Polaritons with two-dimensional and one-dimensional dispersion have been obtained in QW's and QWW's, respectively, and effects produced on the optical absorption have been experimentally observed.[10-12] Also, the short natural lifetimes which have been theoretically predicted for QW fluorescence have been experimentally observed.[13]

The cases of more complicated mesoscopic structures, such as asymmetric quantum wells (AQW's) is of current interest because new effects may occur and nonlinear properties near the exciton states are enhanced.[14-17] For this case a simplified two-band model has been recently proposed and has been shown to apply for the microscopic calculations of exciton energies and oscillator strengths.[18] The problem of computing the optical response of a composite medium containing asymmetric wells is of interest, but seems to be very difficult because the number of boundary conditions is increased and the plane of specular symmetry which allows a simple treatment of the modes is absent in this case.

We address such a problem using the simplified treatment for the optical response of a composite medium proposed by Agranovich,[19,20] and applied to superlattices,[21] when the wavelength of the radiation is large compared with the period of the superlattice. We will show that dispersion relations and lifetimes of reduced dimension polariton states are obtained, and the case of asymmetric wells can be easily studied. The optical properties can be computed in such cases and the effects due to the mesoscopic structures can be observed in absorption, reflectivity, and transmission experiments.

In Sec. II we recall the general mean-field method and show how the electric field can be connected to the polariton modes by appropriate boundary conditions at all the surfaces which separate different structures. In Sec. III we derive the polariton states in the instantaneous approximation. In Sec. IV we use the method to obtain the polariton states in asymmetric wells and derive the optical properties of materials containing such structures. The main results are discussed in Sec. V, where experiments to verify this theory are also suggested.

II. MEAN-FIELD METHOD FOR ASYMMETRIC MICROSTRUCTURES

A general approach to the calculation of the linear optical response of a composite medium from the susceptibilities of the component mesoscopic structures has been introduced in Ref. 19 (see also Ref. 24). The basic approximation is that the wavelength λ of the electromagnetic field in the sample is larger than the distance over which the potential changes ($L/\lambda \ll 1$, L being the typical QW width or SL period). In that case we can use the approximation of constant electric field, or adopt an expansion in L/λ. In Fig. 1 we show an example of a composite medium in the form of step QW, as well as a schematic representation of the electric-field distribution in the sample.

Let us consider a mesoscopic medium, homogeneous in the $\hat{x}$ and $\hat{y}$ directions and discontinuous in the $\hat{z}$ direction (such as a multiple quantum-well structure with QW's of width L_w separated by a distance $L-L_w$). The linear susceptibility in each region of the sample is nonlocal in the $\hat{z}$ direction and can be computed from the results of the microscopic theory on excitation energies and

0163-1829/94/49(4)/2658(9)/$06.00

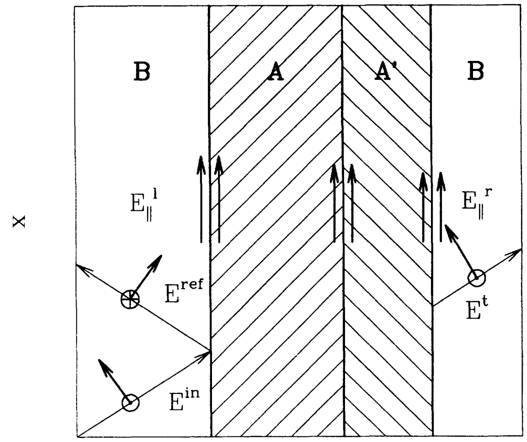

FIG. 1. Schematic representation of a double asymmetric quantum well (A and A') with barriers (B). $E_{\|}^{l}$ and $E_{\|}^{r}$ are the in-plane components of an electric field in the region on the left and on the right of the well. E^{in}, E^{ref}, and E^{t} denote the incident, reflected, and transmitted electric fields of the corresponding electromagnetic waves polarized in the plane of incidence (p polarization) (↑) or perpendicular to it (s polarization) (⊗).

wave functions. Outside the QW regions the susceptibility can be taken as a local function $\chi_B \delta(z-z')$. Inside the QW regions the susceptibility tensor splits into three contributions:

$$\chi(E,z,z')=\chi_b(z)\delta(z-z')+\chi^{el}(E,z,z') +\chi^{es}(E,z,z'), \quad E=\hbar\omega . \tag{1}$$

The first is a background susceptibility, which is often taken to coincide with χ_B, but in general is different, this difference being responsible for interface modes.[22]

The second gives the contribution of the electronic transitions in the continuum between the bands, as obtained from the usual linear-response theory.[23,24] Considering that only the diagonal tensor components can be taken to be different from zero,[24,25] and denoting each pair of subbands with indexes i and j, we have for each polarization p ($p=x,y,z$).

$$\chi_p^{el}(E,z,z')=\sum_{i,j}\chi_p^{el}(i,j,E)A_{ij}(z)A_{ij}(z') , \tag{2}$$

where

$$A_{ij}(z)=A_{ji}(z)=\langle i|z\rangle\langle z|j\rangle , \tag{3}$$

and

$$\chi_p^{el}(i,j,E)=\frac{2e^2P_{pj}^2}{\varepsilon_0 V\omega^2 m_0^2}[f_0(j)-f_0(i)] \times\sum_{k_\|}\left[\frac{1}{E_{ij}(\mathbf{k}_\|)-E-i\Gamma}+\frac{1}{E_{ij}(\mathbf{k}_\|)+E+i\Gamma}\right] . \tag{4}$$

Here, ε_0 is the free-space permittivity, V denotes the QW volume, f_0 is the Fermi function, the confinement factor A_{ij} is the product of the electron and hole envelope functions in state i ($i=1,2,\ldots$) and j ($j=1\beta,2\beta,\ldots$; $\beta=hh,lh$), respectively, and P_{pj} is the bulk dipolar transition-matrix element between states of energy difference

$$E_{ij}(\mathbf{k}_\|)=E_i-E_j+\frac{\hbar^2\mathbf{k}_\|^2}{2\mu_{ij}}, \tag{5}$$

where E_i and E_j denote the bottom electron and the top hole energy levels, and μ_{ij} is their corresponding reduced mass.

The third term of Eq. (1) is the contribution of the exciton bound states inside the quantum well and is given by

$$\chi_p^{ex}(E,z,z')=\sum_{i,j}\chi_p^{ex}(i,j,E)A_{ij}(z)A_{ij}(z') , \tag{6}$$

where

$$\chi_p^{ex}(i,j,E)=\frac{2e^2P_{pj}^2}{\varepsilon_0 L_w\omega^2 m_0^2} \times\sum_{n=1,2}|F_{ij}^{(n)}(0)|^2\left[\frac{1}{E_{ij}^{(n)}-E-i\Gamma_{ex}}+\frac{1}{E_{ij}^{(n)}+E+i\Gamma_{ex}}\right] , \tag{7}$$

each exciton state (n), ($1S,2S,\ldots$) being characterized by the amplitude of the exciton envelope function in the quantum well $F_{ij}^{(n)}(\mathbf{r})$, and the corresponding exciton energies $E_{ij}^{(n)}$.

Following Kane,[3] we can express the bulk momentum matrix elements of light and heavy holes in terms of the average Kane energy E_K as

$$P_{pj}=c_{p\beta}\sqrt{E_K m_0/2}, \tag{8}$$

where $c_{xhh}=1/\sqrt{2}$, $c_{zhh}=0$, $c_{xlh}=1/\sqrt{6}$, $c_{zlh}=\sqrt{2/3}$. Then we perform the $\mathbf{k}_\|$ integration in expression (4), and, using expression (5), obtain the following contribution of the interband continuum:

$$\chi_p^{el}(i,j,E)=c_{p\beta}^2\frac{e^2E_K\mu_{r\beta}}{\varepsilon_0\pi L_w E^2 m_0}[f_0(j)-f_0(i)] \times\int d\epsilon\frac{E_{ij}(\epsilon)}{E_{ij}^2(\epsilon)-E^2-2iE\Gamma}C , \tag{9}$$

where the integration is performed on the subband energy ϵ, and we have taken into account the residual Coulomb interaction between the electrons using the Coulomb enhancement factor $C=\exp(\kappa\pi)/\cosh(\kappa\pi)$, where $\kappa=1/k_\| a_b$, and a_b is the Bohr radius.[26] For the exciton contribution we insert into Eq. (7) the explicit expression of $F^{(n)}(0)$ as given in Ref. 18:

$$F_{ij}^{1S}(0)=\sqrt{2/\pi}\frac{1}{\lambda_{ij}}, \quad F_{ij}(0)^{2S}=\sqrt{2/3\pi}\frac{1}{3\lambda_{ij}} ,$$

and, neglecting the interaction between different exciton states,[18] we obtain

$$\chi_p^{\rm ex}(i,j,E)=c_{p\beta}^2\frac{4e^2E_K\hbar^2}{\varepsilon_0\pi L_w E^2 m_0\lambda_{ij}^2}\times\sum_{n=1,2}\frac{1}{27^{n-1}}\frac{E_{ij}^{(n)}}{E_{ij}^{(n)2}-E^2-2iE\Gamma_{\rm ex}}\ , \tag{10}$$

where λ_{ij} denotes the Bohr radius of the exciton between the two bands i and j.

The microscopic quantum theory of the electronic states allows us to compute explicitly the expressions (1), (9), and (10). This allows the construction of the constitutive equation of the medium relating the electric induction $\mathbf{D}$ to the electric field $\mathbf{E}(z)$ inside the wells:

$$D_p(z,E)=\varepsilon_b(z)E_p(z)+L_w\sum_{i,j}\chi_p(i,j,E)A_{ij}(z)\langle A_{ij}E_p\rangle\ . \tag{11}$$

Here,

$$\varepsilon_p(z)=1+\chi_b(z) \tag{12}$$

is the background dielectric constant at point z,

$$\chi_p(i,j,E)=\chi_p^{\rm el}(i,j,E)+\chi_p^{\rm ex}(i,j,E) \tag{13}$$

gives the contribution of the interband continuum and excitons in the well, and

$$\langle A_{ij}E_p\rangle=\int_0^{L_w}dz\ A_{ij}(z)E_p(z). \tag{14}$$

Outside the QW's we have

$$D_p(z)=\varepsilon_B(z)E_p(z)\ . \tag{15}$$

At this point we make the constitutive equations (11) very simple by using the approximation that the electric field varies very little on the QW width because $\lambda\gg L_w$. An average electric field can be defined inside the well as

$$\overline{E_p}=\frac{1}{L_w}\int_0^{L_w}dz\ E_p(z)=\frac{1}{L_w}\langle E_p\rangle \tag{16}$$

and an average induction can be obtained with the definition of a dielectric function inside the QW,

$$\overline{D_p}=\frac{1}{L_w}\langle D_p\rangle=\varepsilon_p\overline{E_p}\ . \tag{17}$$

By satisfying the appropriate boundary conditions on $E_\parallel$ and using the average field approximation for the in-plane component $\overline{E_{x(y)}}=E_\parallel$, we obtain the expression for the total in-plane dielectric function:

$$\varepsilon_\parallel=\overline{\varepsilon_b}+\sum_{i,j}\chi_\parallel(i,j,E)\langle A_{ij}\rangle^2\ . \tag{18}$$

In the case of the E_z component (perpendicular to the planes) the boundary conditions and the average field approximation give

$$\overline{D_z}=D_\perp\ , \tag{19}$$

which is constant on the boundary, and

$$\overline{E_z}=\frac{1}{L_w}\langle E_z\rangle\ , \tag{20}$$

which is not constant through the boundary. From the constitutive equation (11) we obtain

$$E_z(z,E)=\varepsilon_b^{-1}(z)D_\perp-L_w\sum_{i,j}\chi_z(i,j,E)A_{ij}(z)\varepsilon_b^{-1}(z)\langle A_{ij}E_z\rangle\ . \tag{21}$$

The only unknown terms are the integrals $\langle A_{ij},E_z\rangle$, which can be computed from the above equation by multiplying by A_{ij} and performing the integration on the z variable. This results in the linear system of equations:

$$\sum_{i,j}[\delta_{i,l}\delta_{j,k}+L_w\chi_z(i,j,E)\langle\varepsilon_b^{-1}A_{ij}A_{kl}\rangle]\frac{\langle A_{ij}E_z\rangle}{D_z}=\langle\varepsilon_b^{-1}A_{kl}\rangle\ , \tag{22}$$

which can be solved to obtain all the values

$$\zeta_{ji}(E)=\langle A_{ij}E_z\rangle/D_z \tag{23}$$

as functions of the energy. This gives immediately the perpendicular dielectric function:

$$\varepsilon_\perp^{-1}(E)=\overline{\varepsilon_b^{-1}}-\sum_{i,j}\chi_z(i,j,E)\langle\varepsilon_b^{-1}A_{ij}\rangle\zeta_{ij}(E)\ . \tag{24}$$

The above analysis allows the calculation of the total effective dielectric functions $\varepsilon_\parallel$ and $\varepsilon_\perp$ from the geometry of the microstructures and the microscopic calculation of the electronic structure. An immediate application of this result is to find the absorption coefficient

$$\alpha_p(E)=\frac{E}{n_B\hbar c}{\rm Im}(\varepsilon_p)\ , \tag{25}$$

where $n_B=\sqrt{\varepsilon_B}$. Index p refers to the polarization of the electric field.

We give in Fig. 2 the absorption coefficient of a typical asymmetric QW when the incident electromagnetic wave is polarized in the plane, or perpendicularly to it, as computed from the above expressions with values of the parameters given in Table I. These values are obtained with the method of Ref. 18, where the x dependence of the anisotropic effective masses and the dielectric mismatch are both included.

As may be seen, the spectrum of α_x contains both heavy-hole and light-hole exciton resonances. In the energy range of the figure, one sees the direct heavy-hole ($i=1$, $j=1hh$) exciton peak E_1HH_1 as well as the analogous light-hole exciton peak E_1LH_1. The weak peaks on the right of these resonance correspond to ($2S$) exciton states. The crossed exciton state ($i=1$, $j=2hh$) is manifested by a relatively weak peak (E_1HH_2). This is because the corresponding dipole moment matrix element is proportional to the overlap integral of state $i=1$ and $j=2hh$, and hence it is smaller than the corresponding one of the direct exciton states (see Table I). The interband continuum included in the calculations by $\chi^{\rm el}$ produces the background stairlike structure of the spectra. The absorption given in Fig. 2 is very close to the experimental absorption in an asymmetric well of the type con-

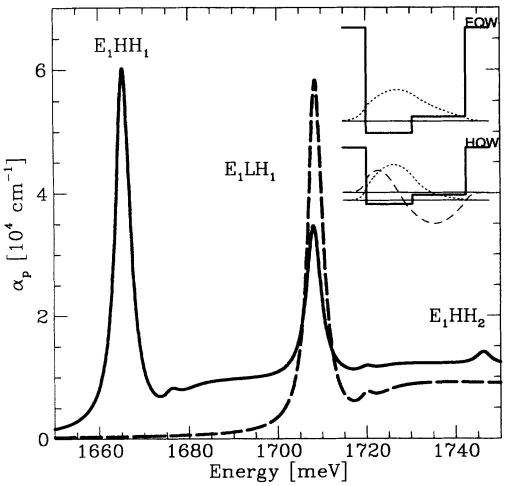

FIG. 2. Absorption spectra at normal incidence of an asymmetric quantum-well structure with AlAs barriers and wells of 3.5 nm of GaAs and 4 nm of $Ga_{0.8}Al_{0.2}As$. The solid line denotes the absorption for an in-plane polarized electromagnetic wave, and the long-dashed line is the corresponding spectrum when the electric field is polarized along the $\hat{z}$ axis. In the inset, the electron (EQW) and hole (HQW) confinement potentials, as well as the first electron level and the first two heavy-hole levels with the corresponding envelope functions, are indicated. The dotted lines refer to the envelope functions corresponding to the two lowest levels, and the short dashed line to the second level. We shall keep these notations for all inserts in the present work. The parameters used in the calculation are given in Table I.

sidered.[27] Experimental evidence of excitations is also obtained from the fluorescence spectrum, but in this case the peaks corresponding to the excitons here reported are a little displayed on the low-energy side (by about 0.1 meV), because emission is proportional to $\mathrm{Im}(\varepsilon_p)$ and absorption is proportional to (25).

As shown by the dipole transition coefficient of Eq. (8), only the light-hole exciton states have a resonance in α_z. This resonance is shifted with respect to its position in the spectrum of α_z by approximately 1 meV, as in the case of symmetric QW. Such a splitting has been considered in the usual optical analysis, on the excitons,[28] and has been found to be due to the electron-hole exchange interaction. This is understood in our procedure as due to the fact that the parallel electric-field components do not change across the internal surfaces, and the perpendicular one changes according to the boundary conditions as in (24). Thus, an AQW may be considered as a point microstructure in the case of an in-plane electric field, and as a condensed medium with some internal charge distribution in the case of a $\hat{\mathbf{z}}$-polarized electromagnetic wave.

The above results remain valid for a superlattice with narrow minibands, except for the fact that the average has to be performed over the superlattice period L, and the susceptibility χ must be multiplied by L_w/L.

In case we have a number of QW's with a barrier region of a thickness comparable with the light wave length, we must consider separately the dielectric functions for the barrier and for each quantum well and obtain the optical properties by considering all boundary conditions with the transfer-matrix approach.

III. INSTANTANEOUS POLARITONS

The procedure described above is appropriate to derive the optical properties of a composite medium, but it does not give details such as the spatial dispersion of the polariton states. To obtain these effects we must consider explicitly the wave-vector dependence of the exciton states into Eq. (10), i.e.,

$$E_{ij}^{(n)}(K_\parallel)=E_i-E_j+R_{ij}^{(n)}+\hbar^2K_\parallel^2/2(m_e+m_j)\ , \tag{26}$$

where $R_{ij}^{(n)}$ is the binding energy of the (n) ij exciton state. We must also consider the wave vector of the radiation in the barrier $Q=\sqrt{\varepsilon_B}\,\omega/c$. In such a way, the exciton susceptibility χ_p^{ex} of Eq. (7), and hence the dielectric functions $\varepsilon_\parallel$ of Eq. (18) and $\varepsilon_\perp$ of Eq. (24) become dependent on the in-plane component of the exciton wave vector $K_\parallel$. Taking into account the above expressions for $\varepsilon_\parallel$ and $\varepsilon_\perp$, we may apply the standard approach in order to obtain the reflectivity coefficients of an asymmetric quantum well. As a first approximation, we may consider reflection only from the surface between the barrier and the quantum well (for example, the boundary between regions B and A in Fig. 1). That model corresponds to the case of reflectivity from a semi-infinite anisotropic medium represented by its parallel and perpendicular dielectric function. Thus, following Drude,[29] we find

$$r_s=\frac{n_BK_z-(Q^2\varepsilon_\parallel-\varepsilon_BK_\parallel^2)^{1/2}}{n_BK_z+(Q^2\varepsilon_\parallel-\varepsilon_BK_\parallel^2)^{1/2}} \tag{27}$$

and

$$r_p=\frac{n_\parallel n_\perp n_BK_z-\varepsilon_B(Q^2\varepsilon_\perp-\varepsilon_BK_\parallel^2)^{1/2}}{n_\parallel n_\perp n_BK_z+\varepsilon_B(Q^2\varepsilon_\perp-\varepsilon_BK_\parallel^2)^{1/2}}, \tag{28}$$

TABLE I. Calculated exciton parameters for an asymmetric quantum well with AlAs barriers and GaAs ($L=3.5$ nm)-$Ga_{0.8}Al_{0.2}As$ ($L=4$ nm) wells. The theoretical model and material parameters used in the calculations are computed as indicated in Ref. 18. The temperature is $T=4$ K.

(i,j)	$E_{ij}^{(1S)}$ (meV)	$R_{ij}^{(1S)}$ (meV)	$R_{ij}^{(2S)}$ (meV)	$\lambda_{ij}^{(1S)}$ (nm)	$\langle A_{ij}\rangle$
E_1HH_1	1665.4	12.6	1.7	10	0.97
E_1HH_2	1746.3	11	1.6	11.1	0.21
E_1LH_1	1708.2	13.9	2	8.9	0.99
E_1LH_2	1849.8	11.7	1.8	10.2	0.08

where $\varepsilon_{\parallel}$ and $\varepsilon_{\perp}$ are given, respectively, by Eqs. (18) and (24), $K_z=\sqrt{Q^2-K_{\parallel}^2}$, and $n_{\parallel(\perp)}=\sqrt{\varepsilon_{\parallel(\perp)}}$ denotes the corresponding refractive index. Here, r_s is the reflection coefficient for an electromagnetic wave when the electric field is perpendicular to the plane of incidence (s polarization), and r_p is the reflection coefficient when the electric field lies in the plane of incidence (p polarization). The angle of incidence θ is defined by $\sin(\theta)=K_{\parallel}/Q$. From the above two expressions, according to the general results of scattering theory,[30] we find the states $E(K_{\parallel})$ in correspondence to poles in r_s and r_p. These eigenstates result from the mixing of the electromagnetic field and the quantum-well exciton states without retardation ($c\to\infty$). The resonant states of r_s (the poles of $\varepsilon_{\parallel}$) correspond to the so-called transverse modes (T modes), because the electric field is perpendicular to the plane of incidence. Their dispersion law $E^T(K_{\parallel})$ coincides with that of the corresponding exciton energies, i.e.,

$$E_{ij}^T(K_{\parallel})=E_{ij}^{(n)}(K_{\parallel}) \ . \tag{29}$$

Analogously, the resonances in r_p give two types of resonant states; one corresponds to the longitudinal modes (L modes) and occurs for $\varepsilon_{\parallel}(E,K_{\parallel})=0$, which in the approximation under consideration coincides with Eq. (29); the second type of resonance coincides with the poles of $\varepsilon_{\perp}^{-1}$ (Z modes) and their dispersion law can be found from the following equation:

$$\varepsilon_{\perp}(E,K_{\parallel})=0 \ . \tag{30}$$

We show in Fig. 3 the reflectivity spectra of the same asymmetric quantum well whose absorption at $K_z=0$ was reported in Fig. 2. We can observe that the light-hole exciton structure in r_p is displaced towards high energy, because of the contribution of the z component. The crossed exciton state (E_1HH_2) appears as a small peak as in the case of absorption. As can be seen from relations (27) and (28), the reflectivity spectra change with the angle of incidence and give the dispersion curves of the models L, T, and Z of the instantaneous polaritons, as function of $K_{\parallel}$. The first two are given immediately by Eq. (29), where in the approximation so far adopted, the splitting between the L and T modes is negligible. The dispersion law of the Z mode obeys a simple analytical expression obtained from the solution of (22) near a fixed resonance,

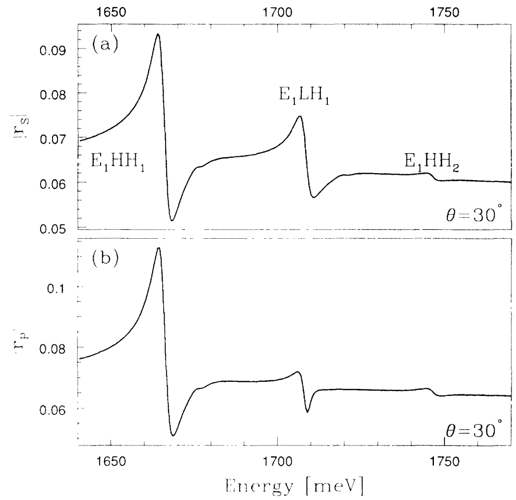

FIG. 3. Reflectivity at the surface of a single asymmetric quantum well with sample parameters of Table I as in Fig. 2. Cases (a) and (b) refer to parallel and perpendicular polarization, respectively, with an angle of incidence of 30°.

$$\varepsilon_{\perp}(E,K_{\parallel})=\frac{L_w}{\langle\varepsilon_b^{-1}\rangle}+\frac{L_w^2}{\langle\varepsilon_b^{-1}\rangle^2}\sum_{i,j}\frac{\chi_z(E)\langle\varepsilon_b^{-1}A_{ij}\rangle^2}{1+L_w\chi_z(E)(\langle\varepsilon_b^{-1}A_{ij}^2\rangle-\langle\varepsilon_b^{-1}A_{ij}\rangle^2/\langle\varepsilon_b^{-1}\rangle)} \ . \tag{31}$$

Taking only the exciton part of χ_z and considering the background dielectric permeability as a constant $\varepsilon_b(z)\simeq\varepsilon_B$, we find the solution of Eq. (30) to be

$$E_{ij}^Z=E_{ij}^{(n)}(K_{\parallel})+\frac{1}{\varepsilon_B}\chi_z(i,j)\langle A_{ij}^2\rangle \ , \tag{32}$$

where

$$\chi_z(i,j)=\frac{4e^2P_{zj}^2\hbar^2}{\varepsilon_0(E_{ij}^{(n)})^2m_0^2}|F_{ij}^{(n)}(0)|^2 \tag{33}$$

is responsible for the correction to the exciton dispersion, which in this approximation is independent of $K_{\parallel}$. Here, one may see that the splitting Δ_{ZT} between modes Z and T depends on the z component of the momentum matrix element P_{pj}, and hence is equal to zero for the heavy-hole polariton states. In the case of the AQW shown in Fig. 2 the splitting is approximately 2 meV for the light-hole polariton state (see also Fig. 5). This value is almost twice that reported in Ref. 28 for symmetric 60-Å wide QW mostly because of the higher oscillator strength due to the confinement of the lowest exciton state in the 35-Å-thick layer. For the purpose of displaying the dependence of the Δ_{ZT} splitting on well parameters we give in Table II the computed values for different QW's with lengths and concentrations chosen to be the same as those on which absorption experiments have been carried out by Fröhlich *et al.*[12] It can be observed that the agreement is satisfactory.

In the simple case of a symmetric quantum well for $i=1$ and $j=1lh$ we have for infinite barrier potentials $\langle A_{11lh}^2\rangle\sim3/(2L_w)$ and we find the approximation expression

$$\Delta_{ZT}\sim\frac{3}{2L_w\varepsilon_B}\chi_z(1,1,lh) \ , \tag{34}$$

TABLE II. Splitting between Z and T modes and the corresponding linewidths in a symmetric QW of varying widths for $K_{\parallel} \approx 0.018$ nm^{-1}. The experimental results with angle of incidence $\theta \simeq 43°$ are taken from Fig. 3 of Ref. 12.

L_w (nm)	x (%)	$\Delta_{ZT}^{\text{expt}}$ (meV)	$\Delta_{ZT}^{\text{theor}}$ (meV)	Γ^T [meV]	Γ^z [meV]
5	35	2.1±0.3	1.5	0.13	0.05
6.6	31	1.3±0.3	1.2	0.13	0.05
9	43	0.9±0.2	1.0	0.14	0.06
10	45	0.9±0.1	0.9	0.14	0.06
13	35	0.5±0.1	0.6	0.12	0.05
15	26	0.35±0.1	0.48	0.11	0.04

which agrees with the results of Ref. 28, when the same limit is considered. Since in Ref. 28 the splitting is computed from the exchange interactions, this gives a further confirmation that the long-range electron-hole exchange interaction is equal to the Coulomb correction introduced by Maxwell equations without retardation.

IV. QUANTUM-WELL POLARITONS

The approximation described above of constant field inside the well is not sufficiently accurate to give the polariton states and their natural lifetimes with retardation effect. To this purpose, choosing our frame of reference at the beginning of the quantum well ($z=0$) and the $\hat{x}$ axis along the exciton wave vector $\mathbf{K}_{\parallel}$ (see Fig. 1), we use the following first-order expansion in (L_w/λ) inside the well:

$$\mathbf{F}(L_w)=\mathbf{F}(0)+\frac{\partial F(0)}{\partial z}L_w , \tag{35}$$

where F may be $\mathbf{E}$, $\mathbf{D}$, or the magnetic field $\mathbf{H}$. Then we take the fields inside the well as

$$\mathbf{F}(\mathbf{r},t)=\mathbf{F}(z)\exp[i(\mathbf{K}_{\parallel}\cdot\mathbf{r}_{\parallel}-\omega t)] , \tag{36}$$

where for simplicity we distinguish the fields $\mathbf{F}(\mathbf{r},t)$ from their z-dependent amplitudes $\mathbf{F}(z)$ by their arguments only. Following the method described in Ref. 19 we impose the boundary conditions and from the phase conservation obtain a constant $K_{\parallel}$ through the boundaries. Making use of Eq. (35) and eliminating the derivative with respect of z from $\mathrm{div}(\mathbf{D})=0$, we find

$$D_z^r(0)-D_z^l(0)=-i(\varepsilon_{\parallel}-\varepsilon_B)L_w\mathbf{K}_{\parallel}\cdot\mathbf{E}_{\parallel}^r(0) , \tag{37}$$

where the superscripts r and l refer to the regions on the right and on the left of the AQW, respectively (see Fig. 1). The other boundary conditions on the field components, with expansion (36), give

$$H_z^r(0)=H_z^l(0) , \tag{38}$$

$$\mathbf{E}_{\parallel}^r(0)-\mathbf{E}_{\parallel}^l(0)=i\left[\frac{1}{\varepsilon_{\perp}}-\frac{1}{\varepsilon_B}\right]L_w\mathbf{K}_{\parallel}D_z^r(0) , \tag{39}$$

$$\mathbf{H}_{\parallel}^r(0)-\mathbf{H}_{\parallel}^l(0)=i(\varepsilon_{\parallel}-\varepsilon_B)L_wQ\hat{\mathbf{z}}\times\mathbf{E}_{\parallel}^r(0) . \tag{40}$$

The solutions of Maxwell equations amount to those of Eqs. (37)–(40) with $\varepsilon_{\parallel}$ and $\varepsilon_{\perp}$ given by Eqs. (18) and (24), respectively. The solutions are classified according to the values of the exciton wave vector $K_{\parallel}$ with respect to Q.

A. Radiative modes

In the region $K_{\parallel}<Q$ the component K_z is a real quantity and we may find the solutions of the above system in the form of plane waves. Let us take the electric field as a TE wave which on the left of the QW is given as a sum of an incident and reflected plane wave

$$E_y^l(z)=F[\exp[i(K_zz)]+R_s\exp[i(-K_zz)]] , \tag{41}$$

and on the right as a transmitted wave

$$E_y^r(z)=F[T\exp[i(K_zz)]] . \tag{42}$$

Substituting these equations in system (37)–(40), we find the reflection coefficient R_s to be given by

$$R_s=\frac{iQ^2\eta_{\parallel}}{2\varepsilon_BK_z-iQ^2\eta_{\parallel}} , \tag{43}$$

where

$$\eta_{\parallel}=L_w(\varepsilon_{\parallel}-\varepsilon_B) . \tag{44}$$

Analogously, considering the reflection of a TM wave from the quantum well, we find for the reflection coefficient of a p-polarized electromagnetic wave

$$R_p=\frac{\varepsilon_B^2K_{\parallel}^2\eta_{\perp}+K_z^2\eta_{\parallel}}{2i\varepsilon_BK_z-\varepsilon_B^2K_{\parallel}^2\eta_{\perp}+K_z^2\eta_{\parallel}} , \tag{45}$$

where

$$\eta_{\perp}=L_w\left[\frac{1}{\varepsilon_{\perp}}-\frac{1}{\varepsilon_B}\right]. \tag{46}$$

In Fig. 4 we give the above-calculated reflection coefficients and compare them with the corresponding ones calculated in the preceding section. One may see that the curves are quite similar but the absolute values of the reflection coefficients are different. They are lower in this case because $L_w<\lambda$ and, as may be seen, R_s/r_s, $R_p/r_p\approx 2L_wQ<1$. Between the exciton peaks, the reflectivity spectra are determined by χ^{el} and $\varepsilon_b(z)$. It is worthwhile to note the contribution of the dielectric mismatch to the magnitude of the reflectivity coefficients. As is shown in Fig. 4, this contribution increases approximately twice the values of R_s and R_p with respect to the corresponding ones when $\varepsilon_b(z)$ is taken to be a constant $[\varepsilon_b(z)=\varepsilon_B]$.

Following the same approach as in Eq. (31) we find

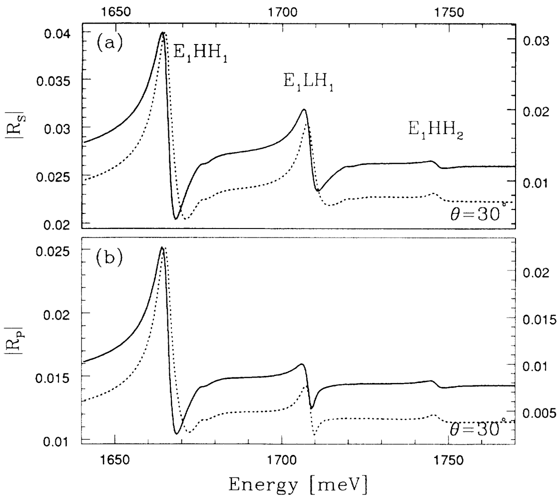

FIG. 4. Reflectivity of a single asymmetric QW described in Fig. 2 including retardation. The angle of incidence $\theta=30°$. The solid lines which refer to the corresponding left-hand scales give (a) the reflection coefficients for s-polarized wave (R_s), and (b) the corresponding coefficient (R_p) for electromagnetic waves polarized perpendicularly to the plane of incidence. The dotted lines which refer to the corresponding right-hand scales give the same spectra as above, but the dielectric mismatch is not taken into account [$\varepsilon_b(z)=\varepsilon_B$].

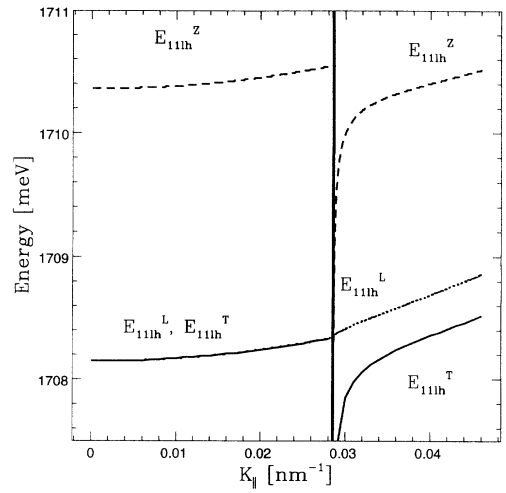

FIG. 5. Dispersion curves of resonant and surface light-hole polaritons in the same steplike asymmetric quantum well as in Fig. 2. The vertical line indicates the photon dispersion $E=\hbar cQ/n_B$.

analytical expressions for the poles of R_s and R_p. As may be seen from Eq. (43) and (45) they are complex quantities of the form $E(K_\parallel)-i\Gamma(K_\parallel)$, so that the effect of reflection is to introduce a natural lifetime of the polariton states. The real parts of these poles in our first-order expansion of the fields coincide with Eqs. (29) and (30) found in the preceding section and give the dispersion laws of the polariton states. This is displayed in Fig. 5 on the left-hand side of the optical line corresponding to $K_\parallel=Q$. The imaginary parts give the corresponding radiative line widths, and can be explicitly written as follows:

$$\Gamma_{i,j}^{T}=\frac{Q^2}{2\varepsilon_B K_z}\chi_\parallel(i,j)\langle A_{ij}\rangle^2 , \tag{47}$$

$$\Gamma_{i,j}^{L}=\frac{K_z}{2\varepsilon_B}\chi_\parallel(i,j)\langle A_{ij}\rangle^2 , \tag{48}$$

and

$$\Gamma_{i,j}^{Z}=\frac{K_\parallel^2}{2\varepsilon_B K_z}\chi_\perp(i,j)\langle A_{ij}\rangle^2 . \tag{49}$$

We show in Fig. 6 the computed values and their $K_\parallel$ dependence of these radiative line widths for the same AQW considered so far. One may see the rapid divergence of modes Z and T as $K_\parallel$ tends to Q. This is also a typical feature of symmetric QW's[8] and can possibly be removed by considering the interaction with wave-guide modes due to dielectric mismatch[22] or performing the calculation in polariton-pole approximation.[23]

Differently from the case of symmetric QW's, in AQW's the indirect exciton states are optically active, and hence they form bound states with photons, one of which can be seen, for instance, as a peak (E_1HH_2) in the absorption spectra of Fig. 2. We shall call these bound states crossed (indirect)[32,33] polaritons. We present in Fig. 7 the cross polariton state from the second light-hole band ($i=1$, $j=2lh$) in the case of an asymmetric double QW. As may be seen from the figure, the Z-T splitting is about 1 meV, which is of the same order of magnitude as Δ_{ZT} of the direct polariton state (2.4 meV in this case). That is because the splitting depends on the square of the confinement factor A_{ij} [see Eq. (32)], which is comparable with that of the direct polariton state in the asymptotic case, and on the exciton oscillator strength, which is also comparable to that of the direct exciton in this asymmetric potential. On the other hand, the radiative line

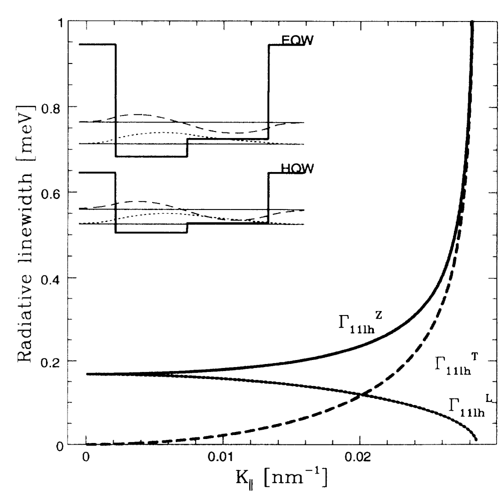

FIG. 6. Radiative linewidths of resonant light-hole polariton modes in the steplike QW already considered. The lowest two electron and light-hole levels are indicated in the inset with their envelope functions.

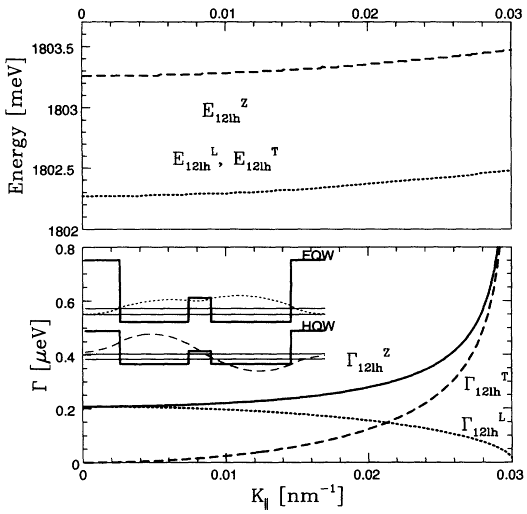

FIG. 7. Crossed light-hole polaritons in double asymmetric QW with AlAs barriers, 3 nm of GaAs, 1 nm of $Ga_{0.5}Al_{0.5}As$, and 3.5 nm of GaAs. The wave functions of the second light-hole and the first electron bound state are shown in the inset. The inset notations are as in Fig. 2.

widths depend on A_{ij} [see Eqs. (47)–(49)]. Here, the different symmetries of states i and state j provide very small values of Γ^Z, Γ^T, and Γ^L, and hence very large lifetimes ($\tau=\hbar/\Gamma$), even near the divergence point $K_{\|}=Q$. That observation is demonstrated in Fig. 7, where the crossed polariton line widths are about three orders of magnitude smaller than in the case of direct polariton states. This extends the exciton study of double wells in an electric field.[32]

B. Surface quantum-well polaritons

In the region $K_{\|}>Q$, K_z is an imaginary quantity and we are looking for solutions localized in the $\hat{z}$ direction of the type of evanescent waves

$$F_p(z)\propto \exp[-|K_z z|] \ . \tag{50}$$

In this case the condition for nonzero solutions of the Maxwell equations gives the same equations as in the preceding section but K_z is replaced by iK_z. As a consequence, we obtain real eigenvalues, which formally coincide with the poles of R_s and R_p from evanescent fields. The dispersion laws of T modes are determined from the equation

$$2\varepsilon_B K_z + q^2\eta_{\|}=0 \ , \tag{51}$$

and those of L and Z modes from

$$2\varepsilon_B K_z + \varepsilon_B^2 K_{\|}^2\eta_{\perp} + K_z^2\eta_{\|}=0 \ , \tag{52}$$

the radiative line widths being equal to zero.

Substituting expressions (18) and (31) for $\varepsilon_{\|}$ and $\varepsilon_{\perp}$, which is consistent with our first-order expansion in $(K_{\|}L_w)$, we find the following explicit expressions for the dispersion relations of the surface polariton states:

$$E_{i,j}^{T}=E_{ij}(K_{\|})-\frac{Q^2}{2\varepsilon_B K_z}\chi_{\|}(i,j)\langle A_{ij}\rangle^2 \ , \tag{53}$$

$$E_{i,j}^{L}=E_{ij}(K_{\|})+\frac{K_z}{2\varepsilon_B}\chi_{\|}(i,j)\langle A_{ij}\rangle^2 \ , \tag{54}$$

$$E_{i,j}^{Z}=E_{ij}(K_{\|})+\frac{1}{\varepsilon_B}\chi_z(i,j)\left[\langle A_{ij}^2\rangle-\frac{K_{\|}^2}{2K_z}\langle A_{ij}\rangle^2\right] . \tag{55}$$

The dispersive behavior of the surface polariton states is shown on the right-hand side of the photon line $E=\hbar cQ/n_B$ and $K_{\|}=Q$, and is displayed in Fig. 5 for the asymmetric well we have considered. One can observe the asymptotic behavior of modes T and Z towards the photon line, while the longitudinal mode L remains continuous in accordance with relations (29) and (54) with $K_z=0$. The radiative linewidths are zero for the surface modes and diverge in the region of radiative polaritons as shown in Fig. 6. Hence the resonant modes Z and T are in practice inactive for $K_{\|}=Q$, but become surface modes with an infinite lifetime for $K_{\|}>Q$, similarly to the case of symmetric QW's.[8] The role of the asymmetry is in the magnitude of the effects and in the appearance of the crossed polariton modes.

V. DISCUSSION AND CONCLUSION

We have presented a theoretical model which allows the calculations of the polariton states of AQW's of arbitrary shape. The reflectivity, transmission, and other optical properties can all be obtained as functions of the exciton states and of the computed averaged dielectric functions $\varepsilon_{\|}$ and $\varepsilon_{\perp}$.

The absorption spectra give the possibility to study the direct as well as the crossed exciton transitions in an AQW. Experiments at an angle of incidence with perpendicular and parallel polarization[12] can be interpreted, and give information on the splitting between the light-hole Z and T, which are in agreement with our results, as shown in Table II.

The reflectivity spectra contain the full information on the polariton states. As was shown in Sec. IV, the Z-T splitting occurs for the light-hole polaritons, and the surfacelike polariton modes are separated from resonant modes by the photon line. Dispersion laws and lifetimes have been given for AQW's of all shapes. Experimental evidence for these modes can be obtained with the use of grating or a ZnSe prism in optical contact with the sample (see Fröhlich and co-workers[12,31]). In the case of surface polaritons, a prism with an index of refraction greater than that of the barrier material is needed to excite surface modes and to produce attenuation reflectance.[8]

The crossed polaritons are present in AQW's; their influence in the reflectivity spectra is small because of the small transition dipolar momentum. Another possibility for observation may be the two-photon absorption. In fact, a very particular feature of the crossed polaritons is their large contribution to nonlinear optical effects, as we have demonstrated with this approach and will show explicitly in further work.

The results here obtained are a natural continuation of the studies on polariton states in symmetric quantum wells and superlattices. The theoretical model gives a unique and simple approach to calculate the optical properties of asymmetric quantum wells and may be extended to other mesoscopic structures as gratings of asymmetric QWW's and dots.

ACKNOWLEDGMENTS

The authors are indebted to Dr. Paolo Giannozzi for his help in the numerical calculations, and to Y. Chen and A. Tredicucci for communicating their results before publication. Thanks are also due to Dr. Giuseppe La Rocca for useful suggestions. One of the authors (V.M.A.) wishes to thank Scuold Normale for hospitality.

---

[1] *Heterojunctions and Semiconductor Superlattices*, edited by G. Allan, G. Bastard, N. Boccara, M. Lanno, and M. Voos (Springer-Verlag, Berlin, 1985).

[2] H. Haug, in *Optical Nonlinearities in Instabilities in Semiconductors*, edited by Haug Harmut (Academic, New York, 1988).

[3] G. Bastard, *Wave Mechanics Applied to Semiconductor Structures* (Les Editions de Phisique CNRS, Paris, 1988).

[4] U. Bockelmann and G. Bastard, Europhys. Lett. **15**, 215 (1990).

[5] A. D'Andrea and R. Del Sole, Solid State Commun. **74**, 1121 (1990).

[6] A. D'Andrea and R. Del Sole, Phys. Rev. B **41**, 1413 (1990); A. Tredicucci, Y. Chen, F. Bassani, J. Massies, C. Deparis, and G. Neu, Phys. Rev. B **47**, 10 348 (1993).

[7] M. Nakayama, Solid State Commun. **55**, 1053 (1985); M. Nakayama and M. Marsuura, Surf. Sci. **170**, 641 (1986).

[8] F. Tassone, F. Bassani, and L. Andreani, Phys. Rev. B **45**, 6023 (1992).

[9] V. M. Agranovich and O. A. Dubovskii, Pis'ma Zh. Eksp. Teor. Fiz. **3**, 345 (1966) [JETP Lett. **3**, 223 (1966)]; E. Hanamura, Phys. Rev. B **38**, 1228 (1988).

[10] R. Cingolani, M. Leopore, R. Tommasini, I. Catalano, H. Lage, D. Heitmann, K. Ploog, A. Shimizu, H. Sakaki, and T. Ogawa, Phys Rev. Lett. **69**, 1276 (1992).

[11] R. Cingolani and K. Ploog, Adv. Phys. **40**, 535 (1991).

[12] D. Fröhlich, P. Köhler, E. Meneses-Pacheco, G. Khitova, and G. Weimann, in *Optics of Excitons in Confined Systems*, Proceedings of the International Meeting, Italy, 24–27 September 1991, edited by A. D'Andrea, R. Del Sole, R. Girlani, and A. Quattropani, IOP Conf. Proc. No. 123 (AIP, New York, 1992).

[13] B. Deveaud, F. Clerot, N. Roy, K. Satzke, B. Sermage, and D. S. Katzer, Phys. Rev. Lett. **67**, 2355 (1991).

[14] L. Tsang, S. Chuang, and S. Lee, Phys. Rev. B **41**, 5942 (1990).

[15] L. Tsang and S. Chang, Phys. Rev. B **42**, 5229 (1990).

[16] P. Bois, E. Rosencher, J. Nagle, E. Martinet, P. Boucaud, F. H. Juluen, D. D. Yang, and J-M. Lourtioz, Superlatt. Microstruct. **8**, 369 (1990).

[17] C. Sirtori, F. Capasso, D. Sivco, S. Chu, and A. Cho, Appl. Phys. Lett. **59**, 2302 (1991).

[18] R. Atanasov, F. Bassani, Solid State Commun. **84**, 71 (1992).

[19] V. Agranovch, in *Surface Polaritons*, edited by V. Agranovich and D. Mills, Modern Problems in Condensed Matter Physics Vol. 1 (North-Holland, Amsterdam, 1982).

[20] V. Agranovich, Solid State Commun. **78**, 747 (1991).

[21] V. Agranovich and V. Kravtsov, Solid State Commun. **55**, 85 (1991).

[22] S. Jorda, *Proceedings of the Third International Conference on Excitons in Confined Systems* (Les Editions de Physique, Paris, in press)

[23] J. Knoester, Phys. Rev. Lett. **68**, 654 (1992).

[24] V. Agranovich and V. Ginzburg, *Crystal Optics with Spatial Dispersion and Excitons* (Springer-Verlag, Berlin, 1984).

[25] L. Andreani, F. Bassani, and A. Pasquarello, in *Symmetry in Nature* (Quaderni della Scuola Normale, Pisol, 1991), p. 19; S. Jörda and U. Rossler, Superlatt. Microstruct. **8**, 481 (1990).

[26] M. Shinada and S. Sugano, J. Phys. Soc. Jpn. **21**, 1936 (1966).

[27] A. Tredicucci and Y. Chen (private communication).

[28] L. Andreani and F. Bassani, Phys. Rev. B **41**, 7536 (1990).

[29] P. Drude, Ann. Phys. (N.Y.) **32**, 584 (1987).

[30] R. Newton, *Scattering Theory of Waves and Particles* (McGraw-Hill, New York, 1966).

[31] D. Fröhlich, R. Wille, W. Schlapp, and G. Weimban, Phys. Rev. Lett. **59**, 1748 (1987).

[32] R. Ferreira, C. Delalande, H. Liu, G. Bastard, B. Etienne, and J. Palmier, Phys. Rev. B **42**, 9170 (1990).

[33] A. Zrenner, P. Leeb, J. Schäfer, G. Böhm, G. Weimann, J. Worlock, L. Florez, and J. Harbison, Surf. Sci. **263**, 496 (1992).